

Supporting Information

A. Cylindrical shockwave evolution with probe delay induced by single fs laser pulse in PMMA

Fig. S1 demonstrates the cylindrical shockwave evolution with probe delay induced by single fs laser pulse in PMMA with fluence of 11.9 J/cm^2 . Filament generated and penetrated into material immediately after fs pulse illuminated the sample surface. Intense ionization has been occurred at probe delay of 1 ns with dense plasma distributed in linear range of more than $100 \mu\text{m}$. After ionization, the cylindrical shockwave expanded in the radial direction with a constant speed of 5.2 km/s .

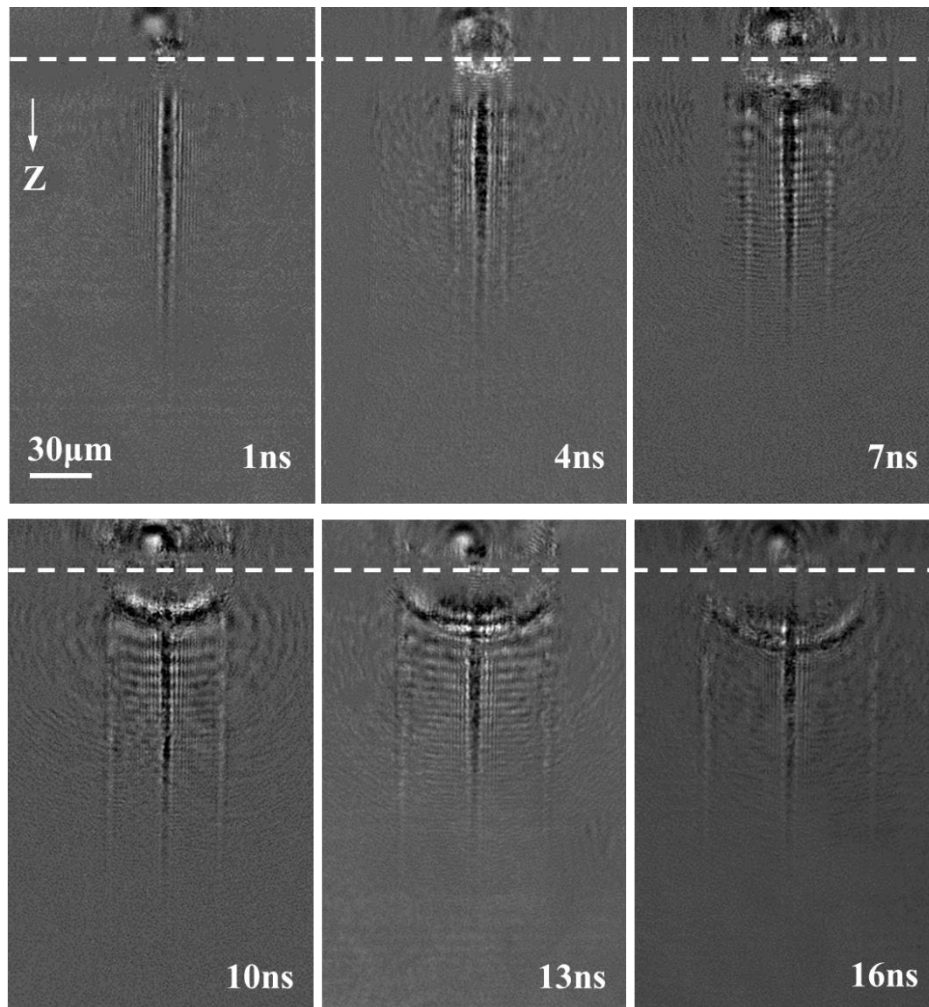


FIG. S1. Cylindrical shockwave evolution with probe delay induced by single fs laser pulse with fluence of 11.9 J/cm^2 . The dashed line represents the surface of the sample and laser propagated from air in the Z-direction.

B. Crater depth evolution with pulse number N.

The crater depths after the first, second, third, fifth, and tenth pulse ablation (N=1, 2, 3, 4, 5, and 10) are shown in Fig. S2. The laser fluence of each pulse was 11.9 J/cm^2 . The error bar is $0.3 \text{ }\mu\text{m}$.

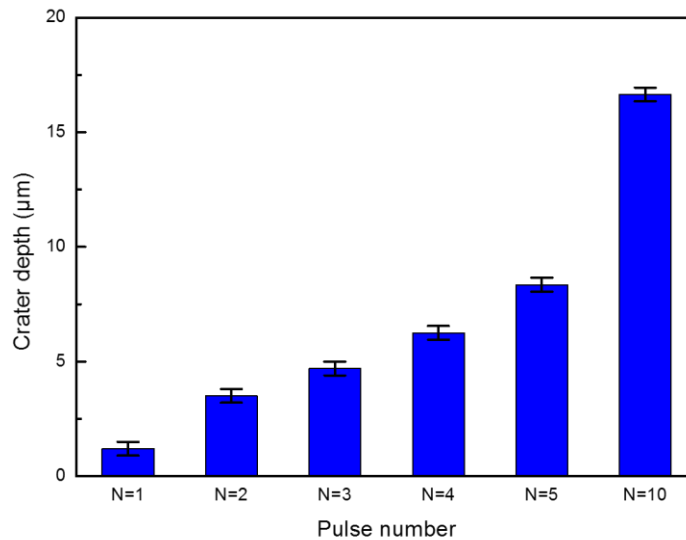


FIG. S2. Crater depth evolution with pulse number N.

C. Morphology contrast of HSW1, HSW2, and CSW generated using single fs laser pulse

The hemispherical shockwave outside the sample (HSW1) was enhanced both in the X- and Z-direction with high power intensity, as shown in Fig. S3 (b).

The enhancement in Z-direction was more obvious from the distorted bulge within the shockwave front. Stronger ionization and more free electrons can be

generated through higher fluence because the multi-photon absorption mechanism of PMMA results in stronger ejection of plasma after the pump pulse in both X- and Z-direction. Additionally, the air break-down channel further contributed to the faster expansion of HSW1 in Z-direction when laser intensity was beyond the threshold of the atmosphere. The expanding distances of HSW2 and CSW (in Z- and X-direction, respectively) were almost invariable with higher pulse energy. The propagation characteristics of HSW2 and CSW were mainly determined by the nature of the material. Therefore, the velocities of HSW2 and CSW remained unaltered when laser intensity increased. However, the electron density and the linear range of ionization in the center of CSW increased with higher laser fluence. As demonstrated in our manuscript, the radial outfield portion of laser pulse was guided deeper into the material. When higher laser intensity was applied, the laser intensity distributed at the boundary of the focus was strong enough to induce sufficient electrons at the front of filament. Thus, the visible ionization range was longer than that induced with low laser intensity.

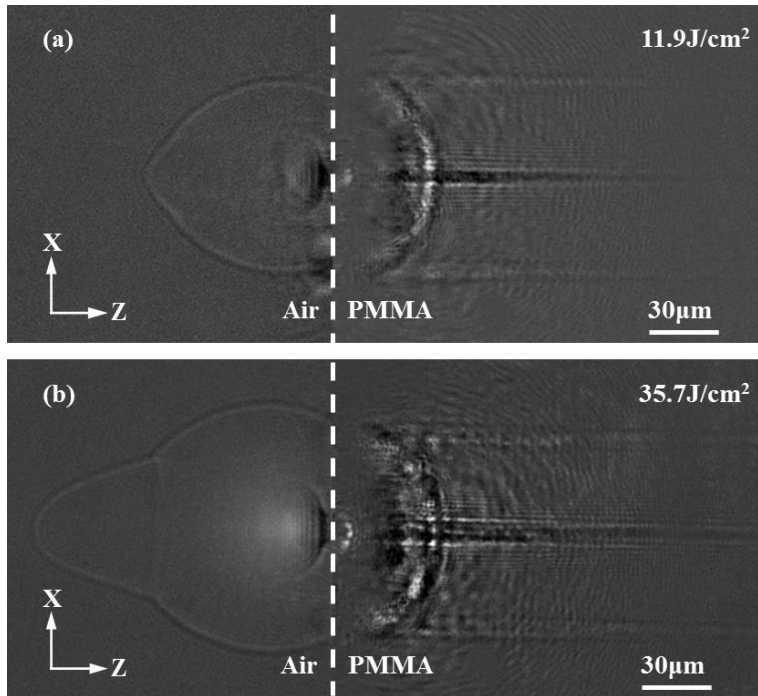


FIG. S3. Morphology contrast of HSW1, HSW2 and CSW generated using single fs laser pulse with laser fluence of (a) 11.9 J/cm^2 and (b) 35.7 J/cm^2 at probe delay of 16 ns.